INVOTEK
Jurnal Inovasi Vokasional dan Teknologi
http://invotek.ppj.unp.ac.id/index.php/invotek

Vol. 25, No. 3, Oct 2025
ISSN: 1411 – 3411 (p)
ISSN: 2549 – 9815 (e)

Numerical Structural Response Analysis of Savonius Wind Turbine Blades with Geometric Variation under Aerodynamic Loads

Aldo Alfattah Sudjono[1], Delima Yanti Sari[1] *, Syahril[1], Rifelino[1]

[1] Department of Mechanical Engineering, Faculty of Engineering, Universitas Negeri Padang
Jl. Prof. Dr. Hamka, Kampus UNP, Air Tawar, Padang, Indonesia-25131

**Corresponding author: delimayanti@ft.unp.ac.id* Doi: https://doi.org/10.24036/invotek.v25i3.1327

Abstract

Rising demand for electrical energy has accelerated the development of renewable energy technologies, including wind turbines designed to operate at low wind speeds. The savonius vertical-axis wind turbine is a promising option due to its simple configuration and insensitivity to wind direction. Nevertheless, the structural reliability of its blades is strongly affected by their geometry and the material selected. This study focuses on evaluating the structural response of savonius turbine blades under aerodynamic loading using the Finite Element Analysis (FEA) method. Simulations were carried out in ANSYS Workbench R2 2025, considering geometric variations in blade thickness (1.2 mm, 1.5 mm, and 2 mm), aspect ratio (0.8, 1.0, and 1.3), and arc angle (120°, 150°, and 180°). The blades were modeled using AISI 304 stainless steel. The analysis examined von mises equivalent stress, total deformation, and safety factor. The analysis results show that all geometric variations are structurally safe with a safety factor value of 15. The highest maximum von mises stress of 0.081 MPa occurs at a thickness of 1.2 mm, while the lowest value of 0.017 MPa is obtained at an arc angle of 180°. The maximum deformation of 3.38×10^{-3} mm occurred at an arc angle of 150°, while the lowest deformation of 6.77×10^{-4} mm was obtained at an arc angle of 180°, which indicates the most structurally stable configuration.

Keywords: Savonius Turbine, Finite Element Analysis, AISI Stainless Steel 304, Static Simulation, Structural Response.

1. Introduction

Electricity demand in Indonesia continues to increase in line with population growth and economic activity, driving the development of environmentally friendly and sustainable renewable energy sources. Wind energy is one of the renewable energy sources with high development potential due to its natural and sustainable nature [1]. As an archipelagic country in the equatorial region, Indonesia has wind energy potential in both onshore and offshore areas, although the characteristics of the wind are generally low speed and unstable, with an effective speed above 2.5 m/s [2], [3].

Under these conditions, vertical axis wind turbines (VAWTs) are considered more suitable because they can operate at low wind speeds and receive airflow from various directions [4]. One type of VAWT that has been widely developed is the savonius turbine, which has a simple design, high starting torque, and the ability to operate in low winds without depending on wind direction [5], [6]. However, the energy conversion efficiency of savonius turbines is still relatively low, at around 15–25% [7], [8].

The main problem with savonius turbines lies in the blades, which bear the aerodynamic load directly. Uneven force distribution during rotation can cause stress concentration and local deformation, which can potentially lead to material fatigue and structural failure if the geometric design and materials are not suitable [9], [10]. Therefore, structural analysis is required to evaluate the blade's response to the aerodynamic loads acting on it.

Finite element analysis (FEA)-based static analysis is commonly employed to assess the stress distribution, deformation, and safety factors of structures subjected to equivalent loads [9]. This method

Received date 03/02/2026, Revised date 17/03/2026, Accepted date 09/04/2026

P-ISSN: 1411-3414
E-ISSN: 2549-9815

can also be applied to savonius type turbine blades, where aerodynamic load variations during rotation can be represented by equivalent constant loads to study maximum stress conditions [10]. Several previous studies have discussed the influence of geometry and wind speed on blade structural response, with some studies even using materials such as carbon steel and galvalume [10]–[12].

With its high ductility, mechanical stability, and resistance to corrosion, AISI Stainless Steel 304 is an austenitic stainless steel that may increase the dependability of turbine blades used in outdoor settings [13]. However, there are currently few numerical studies on the structural response of savonius turbine blades made of stainless steel 304 with different geometries. These studies focus on the impact of arc angle, aspect ratio, and blade thickness on stress, deformation, and safety factors using the FEA approach.

Based on this, this study aims to analyze the structural response of savonius turbine blades made of AISI Stainless Steel 304 using the finite element analysis (FEA) method, focusing on the effect of blade geometry variations on von mises stress, total deformation, and safety factors based on aerodynamic loads resulting from flow simulations.

To clarify the contribution of this study, it should be emphasized that previous studies generally focused more on aerodynamic optimization or conducted structural analysis using different materials such as carbon steel, galvalume, AISI 1018 and 1020, as well as composite materials like fiberglass. This study adopts a different approach by focusing the analysis on AISI Stainless Steel 304 and integrating computational fluid dynamics (CFD) simulation results as the source of aerodynamic loading into a finite element analysis (FEA)-based structural analysis.

In addition, this research systematically analyzes the savonius turbine model developed by the authors by evaluating the effect of blade geometry variations, including arc angle, aspect ratio, and blade thickness, on the resulting structural response. This approach enables the establishment of a relationship between geometric parameters and stress response specifically for SS 304 in savonius turbines. Therefore, this study not only provides the structural response of the blades but also offers design insights and recommendations for more suitable geometric configurations for small-scale savonius turbine applications under low wind conditions.

1.1 Savonius Vertical Axis Wind Turbine (VAWT)

Wind turbines convert wind kinetic energy into mechanical energy through shaft rotation [14]. Based on the orientation of the rotating axis, wind turbines are classified into horizontal axis wind turbines (HAWT) and Vertical Axis Wind Turbines (VAWT), where VAWTs are capable of operating in unstable wind directions and speeds [8]. The savonius turbine is a simple type of VAWT introduced by savonius in 1922, using "S"-shaped semi-cylindrical blades and working on the principle of drag force [8], [15]. The difference in drag force between the advancing and returning blades produces rotational torque. Although it has good self-starting capabilities at low wind speeds, the efficiency of the savonius turbine is relatively low, at around 15% [8], [16]. Structural response analysis is required to guarantee turbine reliability because aerodynamic loads acting directly on the blades can result in stress and deformation [17].

1.2 Blades

The primary parts of savonius wind turbines that harness wind energy and transform it into mechanical force acting on the rotor are the blades. Wind speed and the shape and geometry of the blades used both have a significant impact on the speed at which the blades, which are attached to therotor, rotate as a result of their direct interaction with the wind flow [8].

The drag force created when wind passes over the blade surface is the main source of power for the blades in savonius turbines. The torque produced by this drag force turns the turbine rotor. The turbine operating conditions and blade design have an impact on the force's magnitude [18]. Variations in blade geometry therefore have a significant impact on the structural response and turbine performance. In order to optimize interaction with wind flow, savonius turbine blades are typically positioned perpendicular to the rotor shaft [19].

P-ISSN: 1411-3414
E-ISSN: 2549-9815

1.3 AISI Stainless Steel 304

Because a passive layer forms on the surface of AISI stainless steel 304 (SS 304), an austenitic stainless steel based on a chromium–nickel (Cr–Ni) alloy, it has good corrosion resistance [20]. Because of its high ductility, ease of fabrication and welding, and mechanical stability, this material finds extensive use in both structural and industrial applications [20]–[22].

With a very low ferrite content and a predominance of the austenite phase in its microstructure, SS 304 exhibits ductile elastic-plastic behavior and can withstand mechanical loading without breaking easily [20]. These characteristics make it possible to accurately model SS 304 in numerical analysis based on finite element analysis (FEA), especially when assessing stress, deformation, and safety factors.

1.4 Finite Element Analysis (FEA)

By breaking down the geometry into small elements (mesh), finite element analysis (FEA) is a numerical technique for examining how structures behave under specific loads. This allows for the computational calculation of the stress and deformation distribution [23]. This method is commonly used in the design stage to evaluate structural performance prior to fabrication and reduce the risk of failure [24]. Mathematically, FEA solves boundary value problems that represent the physical conditions of the structure [10]. In wind turbine blade analysis, FEA is used to efficiently evaluate the structural response to aerodynamic loads [23].

1.5 Von Mises Stress

Von mises stress is a material failure criterion used to evaluate the yielding condition of materials under multiaxial loading. This theory was first introduced by Huber (1904) and later developed by Von Mises and Hencky, who stated that plastic failure occurs when the distortion energy generated is equivalent to the distortion energy under the same uniaxial tensile condition of the material. This criterion is expressed in terms of von mises equivalent stress, which is a combination of normal stress and principal shear stress. which is formulated in Equation 1 von mises equivalent stress as follows:

$$\sigma' = \sqrt{\frac{(\sigma_1-\sigma_2)^2+(\sigma_2-\sigma_3)^2+(\sigma_3-\sigma_1)^2}{2}} \tag{1}$$

or, for voltage equations with Cartesian coordinates (x, y, z) with three planes:

$$\sigma' = \sqrt{\frac{(\sigma_x-\sigma_y)^2+(\sigma_y-\sigma_z)^2+(\sigma_z-\sigma_x)^2+6(\tau_{xy}^2+\tau_{yz}^2+\tau_{zx}^2)}{2}} \tag{2}$$

According to [25], a material is considered to be at yield when the von mises stress value is equal to or exceeds the yield stress of the material. In general, the safety of a structure can be assessed by comparing the von mises stress to the yield stress of the material, taking into account the safety factor. Therefore, von mises stress is widely used in finite element analysis (FEA)-based numerical analysis to predict the possibility of plastic deformation and structural failure. Thus, structural failure can be said to occur if,

$$\sigma' \geq \frac{Tensile\ Yield\ Strength}{Safety\ Factor} \tag{3}$$

1.6 Total Deformation

Total deformation is an important parameter in structural analysis to describe changes in the shape and size of a component due to loading. These changes can be in the form of elongation or contraction, depending on the direction and type of force acting on the component [26]. A small total deformation value indicates that the structure has good rigidity and is able to maintain its stability, while a large deformation indicates low rigidity and the potential for structural problems. Deformation can be elastic, meaning that it returns to its original shape after the load is removed, or plastic, which is permanent when the stress exceeds the elastic limit of the material.

Numerically, the total deformation is obtained from the resultant deformation in the X, Y, and Z axes, which is used as the basis for evaluating the structural feasibility of the applied load using the following equation:

P-ISSN: 1411-3414
E-ISSN: 2549-9815

$$\delta_{total} = \sqrt{(\delta X)^2 + (\delta Y)^2 + (\delta Z)^2} \quad (4)$$

1.7 Safety Factor

The safety factor is used to assess the level of safety of a structure against failure due to loading. Failure occurs when the actual stress exceeds the allowable stress, which in clay materials is generally based on the yield strength [27]. The safety factor is defined as the ratio between the load or stress that causes failure and the allowable load or stress. The safety factor value must be greater than one so that the structure has a safety margin against loading uncertainties, fabrication errors, and environmental influences [28]. The safety factor (factor of safety) can also be expressed in the following equation:

$$F.S. = \frac{F_{fail}}{F_{allow}} \quad (5)$$

The selection of safety factor values needs to be adjusted to the type of loading and the level of design uncertainty, because values that are too low increase the risk of failure, while values that are too high can reduce structural efficiency [29].

2. Method

This study is a computational simulation study that uses the finite element analysis (FEA) approach to analyze the structural response of savonius type vertical wind turbine blades to aerodynamic loads. The blade geometry was modeled using solidworks 2024 and analyzed numerically using ANSYS 2025 through the mechanical and fluent modules. The parameters analyzed include von mises stress, total deformation, and safety factors due to wind loading. The turbine design is adjusted to the low wind speed conditions in Padang city, which is 3.6–5.1 m/s with an average of 3.8 m/s and an air density of 1.225 kg/m³. The target power is 10–15 W and the power coefficient is 0.4–0.45. The geometric design refers to several previous studies as the basis for design and numerical validation [30]–[34].

2.1 Vertical Savonius Wind Turbine Design

Figure 1 shows the design of the savonius type vertical wind turbine used in this study, including the main components: the blades, the shaft, and the turbine support. The initial turbine model was designed using CAD with an outer diameter of 300 mm, a height of 910 mm, a blade thickness of 1.2 mm, and other dimensions as shown in Table 1. Geometric parameters such as aspect ratio, thickness, and arc angle are the main variables in this study. This design was used as the basis for modeling in computational fluid dynamics (CFD) and finite element analysis (FEA).

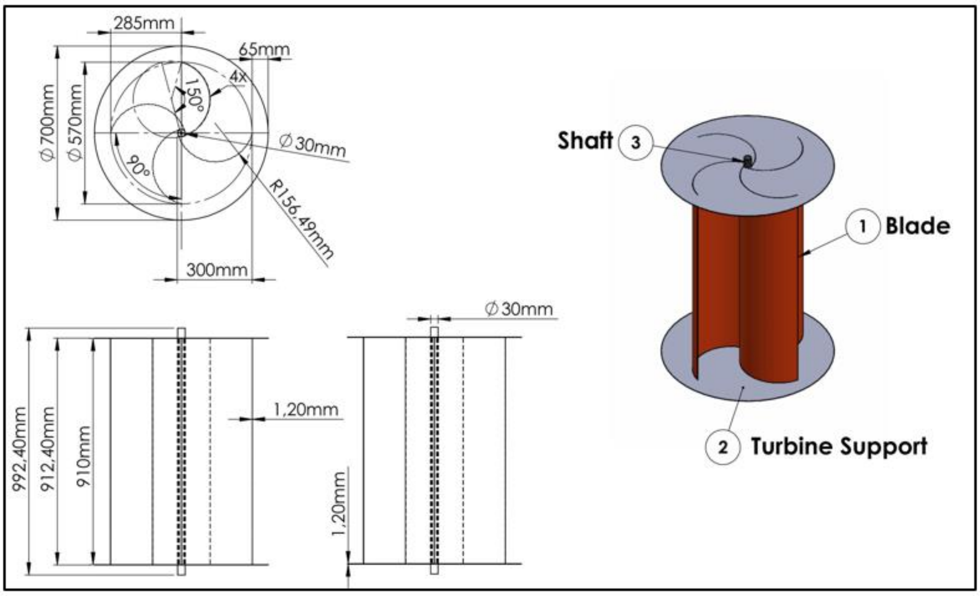

Figure 1. Detail Drawing CAD

P-ISSN: 1411-3414
E-ISSN: 2549-9815

Table 1. Geometric Parameters Savonius Turbine

Parameters	Value
Turbine outer diameter (Do)	700 mm
Turbine inner diameter (D_i)	570 mm
Blade Height (H)	910 mm
Blade width (e)	300 mm
Number of blades	4 pieces
Blade thickness (t)	1.2mm
Blade radius	R155
Blade arc angle	150°
Overlap ratio	0,1
Aspect ratio	1,3
Shaft diameter	30 mm
Blade shape	S or arc

2.2 *Material*

The material used in this turbine study is AISI SS 304, with Table 2, showing the properties of AISI Stainless Steel 304 used as the turbine blade material. These parameters were used as inputs in the structural analysis (FEA) to represent the material's mechanical behavior

Table 2. Material Properties SS-304 Savonius Turbine Blade

Parameters	Value
Density (ρ)	7900 $kg.m^{-3}$
Young's modulus (E)	193.000.000.000 Pa
Poisson's ratio (ν)	0,29
Yield Strength (σ_y)	207.000.000 Pa
Ultimate tensile strength (σ_u)	586.000.000 Pa
Shear modulus	74.806.201.550,3876 Pa
Bulk modulus	153.174.603.174,603 Pa
Coefficient of thermal expansion	1,8E-05 /°C or /K
Melting temperature	1370 °C

2.3 *Geometric Variations*

Figure 2 below shows the geometric variables used in this study, including blade thickness, aspect ratio, and arc angle.

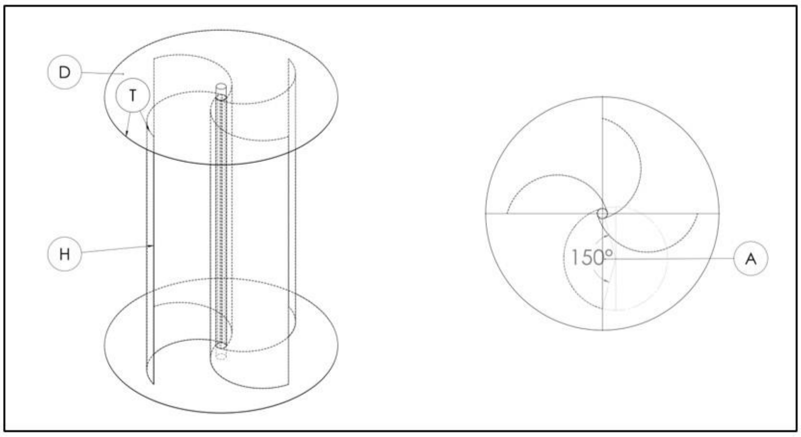

Figure 2. Geometry Variables

P-ISSN: 1411-3414
E-ISSN: 2549-9815

The variations in each parameter are presented in Table 3, along with explanations of the symbols and dimensions for each parameter to be studied, namely blade thickness (T), aspect ratio (H:D), and arc angle (A). These variations are based on previous research and are used to analyze the effect of geometry on the structural response of savonius turbine blades.

Table 3. Geometry Variables Descriptions

Variable	Symbol	Geometric Variations	Value
Blade thickness *Range refers to [23], [33].	T	A.1	1.2 mm
		A.2	1.5 mm
		A.3	2.0 mm
Aspect ratio * Range refers to [12], [35].	H:D	B.1	AR=0.8 : H=560 mm D=700 mm
		B.2	AR= 1 : H=700 mm D=700 mm
		B.3	AR= 1.3 : H=910 mm D=700 mm
Blade curvature (arc angle) *Range refers to [36], [37].	A	C.1	120°
		C.3	180°

2.4 *Simulation Parameters Setup*

In this study, a CFD simulation was performed using ANSYS software before conducting the FEA simulation. To perform the CFD simulation, parameter settings were required so that the simulation results realistically represent the turbine's output behavior in response to the applied load. Details of the simulation parameters used can be seen in Table 4.

Table 4. Parameter Setup CFD Ansys Fluent

Setup	Sub-Setup	Details
Pre-Processing	Modeler	Solidworks 2024 & Ansys spaceclaim
	Geometry	Space: 3D
	Meshing	Ansys fluent meshing
	Model	Time: Steady Type: Pressure-based Velocity formulation: Absolute Viscous: SST k-omega turbulence
Solving	Materials	Fluid: Air Solid: AISI SS 304
	Turbine	Rotation-axis direction (0,1,0) Inlet: Velocity-inlet Outlet: Pressure-outlet Moving wall: yes Frame motion: Relative to adjacent cell zone-rotating Rotation-axis direction (0,1,0)
	Inlet	Velocity magnitude = 3.8 m/s
	Outlet	Condition value pressure outlet = 0 Pa
	Monitor	Report definition plots: Force-X,Y,Z; moment Initialization: Standard Calculation activities: 5 Time Step Method: User-specified Pseudo time step size (s): 0.01

P-ISSN: 1411-3414
E-ISSN: 2549-9815

		Iteration/convergence criteria: 700
Post-Procesing	Output	Pressure distribution Pressure contour

The input parameters in the CFD simulation were kept constant, namely a wind speed of 3.8 m/s. The simulation output was the pressure distribution on the blade surface, which was then exported from ANSYS Fluent and imported into ANSYS Mechanical as a pressure load in the FEA analysis. Although the wind speed was kept constant, the resulting pressure distribution differed for each geometry variation. The pressure load from the CFD results is then used to analyze the effect of blade geometry variations, namely blade thickness, aspect ratio, and arc angle, as shown in input pressure distribution subsection in Figures 4–7 and summarized in Table 5.

Then, an FEA simulation was performed using ANSYS software. The Finite Element Analysis (FEA) simulation parameters and configurations used in the study ensure consistent and representative structural analysis results. Simulation settings include pre-processing, solving, and post-processing stages, ranging from geometry modeling, meshing methods, analysis types, to convergence criteria. All parameters are set systematically so that the structural response of Savonius turbine blades to aerodynamic loads can be analyzed accurately and compared between geometric variations. And Table 5. presents the simulation's parameter setup configuration.

Table 5. Ansys Mechanical FEA Parameters Setup

Setup	Sub-Setup	Details
Pre-processing	Modeler	Solidworks 2024
	Geometry	Space: 3D
	Meshing	Ansys mechanical meshing Type of element: Solid–tetrahedral
	Model	Type of analysis: Static structural Type of solver: Mechanical APDL solver
Solving	Materials	AISI SS 304
	Boundary conditions	Fixed support: Upper and lower shafts
	Loads	Pressure distribution (import from fluent) – 1 body
	Contacts	Bonded contact
	Solution controls	Auto time stepping: Program controlled
	Convergence criteria	Convergence type: Result-based Quantity: Equivalent (von mises) stress (MPa) Tolerance: User–defined (≤ 5%) Convergence condition: Change of von mises stress between iterations
Post-procesing	Output	Total deformation Equivalent (von mises) stress Factor of safety

Before running the simulation, meshing settings were configured to ensure the accuracy and stability of the simulation results. The meshing parameters are shown in Table 6. which lists the meshing parameters used in the finite element analysis (FEA) performed using Ansys Mechanical.

Table 6. FEA Meshing Parameters – Ansys Mechanical

Parameters	Detail
Method	Automatic
Element Order	Program Controlled
Element Size	19 mm
Min. Edge Length	1,2 mm
Span Angle Center	Medium

P-ISSN: 1411-3414
E-ISSN: 2549-9815

Smoothing	Medium

Figure 3. shows a research flowchart illustrating the stages of the research method used, ranging from literature review, determination of geometric variables, CAD modeling, CFD simulation, pressure data transfer, FEA simulation, to analysis of results and drawing of conclusions.

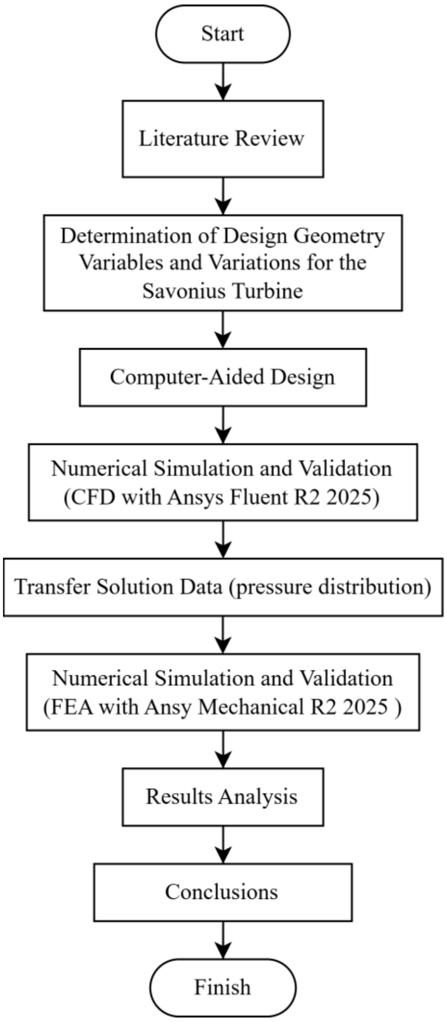

Figure 3. Research Flowchart

2.5 Input Pressure Distribution

In the finite element analysis (FEA) used for the basic structural analysis, the definition of the loads is very important in order to be able to model the real operating conditions. In structures that directly interact with airflow, the dominant load is the aerodynamic pressure exerted on the surface of the structure. This pressure is determined from the results of the computational fluid dynamics (CFD) simulation in the form of surface pressure distribution, which is then used in the FEA analysis as aerodynamic load (imported pressure), as the input parameters have been discussed in the subsection on simulation parameter setup and in Table 4.

The load levels used in this study were designed to represent realistic operating conditions for small-scale savonius wind turbines operating in areas with low wind speeds. Based on meteorological data from the city of Padang and the surrounding area, the average wind speed ranges from 3.6 to 5.1 m/s. This range is also consistent with various studies indicating that savonius turbines can begin operating at low wind speeds, even at speeds above approximately 2.5 m/s. Therefore, the aerodynamic loads used in the simulation were derived from the pressure distribution obtained from computational fluid dynamics (CFD) simulations within this wind speed range, ensuring that the structural response

P-ISSN: 1411-3414
E-ISSN: 2549-9815

analyzed via finite element analysis (FEA) accurately reflects realistic operating conditions for small-scale wind turbine applications.

The selection of this wind speed range is also consistent with the primary objective of the study, which is to design a savonius turbine blade configuration suitable for the low-wind conditions commonly found in Indonesia. Since the intended application is small-scale wind turbines under low-wind conditions, the loading scenarios used focus on operating conditions most relevant to real-world implementation. Thus, the results of this study are expected to provide a realistic structural evaluation of the proposed blade design when subjected to aerodynamic loads under normal operating conditions.

The pressure load results from the CFD are then used to analyze the effect of variations in blade geometry on blade thickness, aspect ratio, and arc angle, as shown in Figure 4–7 and summarized in Table 7.

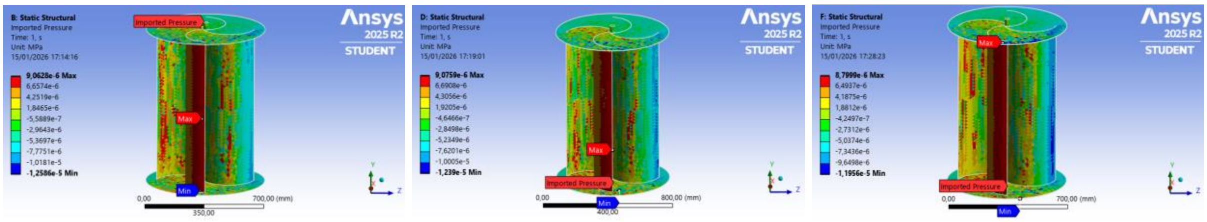

(a) (b) (c)

Figure 4. Imported Pressure on Blade Thickness Geometry; a) 1.2 mm, b) 1.5 mm, c) 2 mm

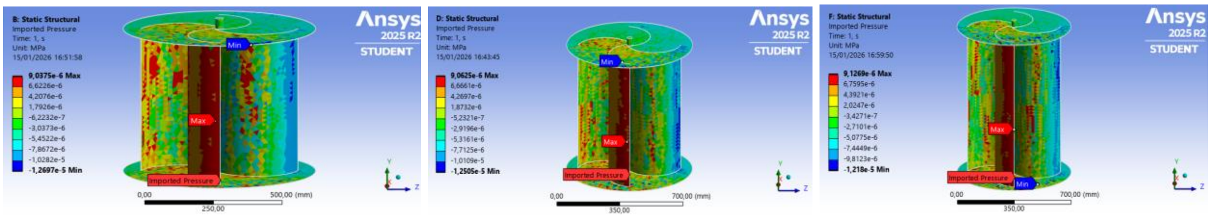

(a) (b) (c)

Figure 5. Imported Pressure on Aspect Ratio Geometry; a) 0.8, b) 1.0, c) 1.3

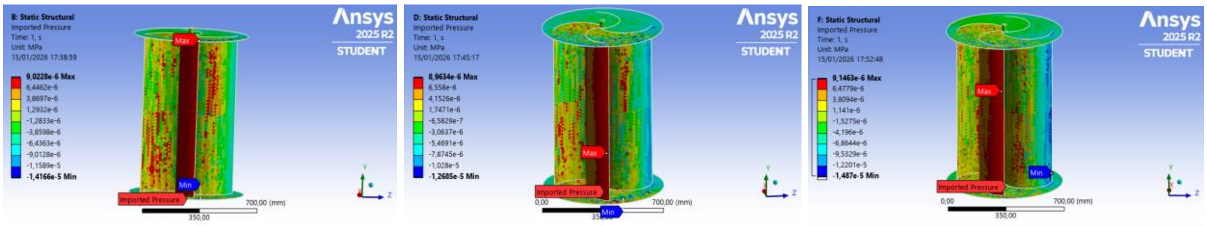

(a) (b) (c)

Figure 6. Imported Pressure on Arc Angle Geometry; a) 120°, b) 150°, c) 180°

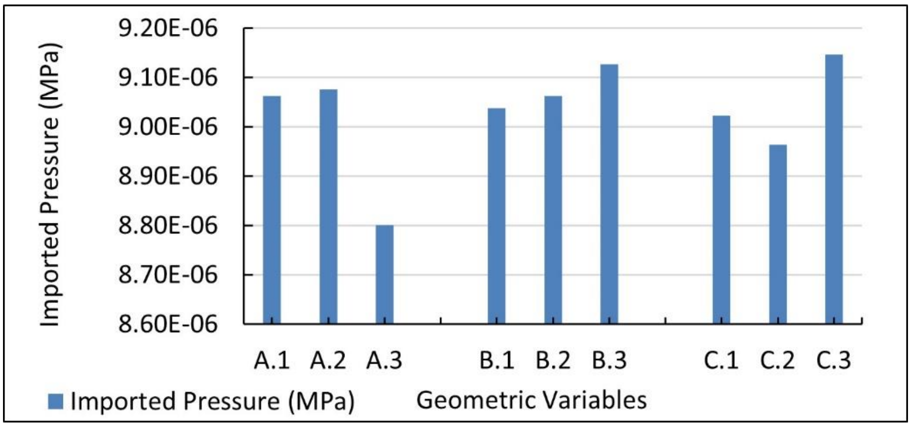

Figure 7. Imported Pressure Diagram as Aerodynamic Load

P-ISSN: 1411-3414
E-ISSN: 2549-9815

Based on Table 7 the aerodynamic pressure used as the FEA load is in the order of 10^{-5} MPa, which is relatively small for structural analysis. The magnitude of the pressure is mainly influenced by the aspect ratio and arc angle, while variations in blade thickness have a relatively small effect on pressure but play an important role in deformation and stress analysis. This CFD pressure is used as imported pressure in FEA to represent more realistic loading conditions in structural strength evaluation.

Table 7. Imported Pressure as Aerodynamic Load

Imported Pressure (MPa)				
Variable	Variation		Min.	Max.
Blade Thickness	A.1	1.2 mm	-1,26E-05	9,0628E-06
	A.2	1.5 mm	-1,24E-05	9,0759E-06
	A.3	2 mm	-1,20E-05	8,7999E-06
Aspect Ratio	B.1	0.8	-1,27E-05	9,0375E-06
	B.2	1	-1,25E-05	9,0625E-06
	B.3	1,3	-1,22E-05	9,1269E-06
Arc angle	C.1	120°	-1,42E-05	9,0228E-06
	C.2	150°	-1,27E-05	8,9634E-06
	C.3	180°	-1,49E-05	9,1463E-06

2.6 Grid Independence Test

The grid independence test is a crucial step in numerical simulations using the finite element analysis (FEA) method to ensure that simulation results are not influenced by the mesh size used. The choice of mesh size affects the accuracy of the analysis results, particularly in predicting key parameters such as von mises stress and total deformation. Therefore, the grid independence test is conducted by varying the mesh size until convergent results are obtained and no significant changes are observed. In this study, the test was performed on a structural model with a plate thickness of 1.2 mm (A.1) using five variations of mesh size, with the primary parameter observed being the maximum von mises stress. The test results are presented in Table 8.

Table 8. Grid Independence Test

Mesh Size (mm)	Number of Elements	Von Mises Stress (MPa)	Difference (%)
28.5	27820	0.043276	-
26	31544	0.057146	24.27116509
23.5	36878	0.077327	26.09825805
21	43277	0.081954	5.645850111
19	48726	0.081006	1.170283683

The results of the grid independence test show that as the mesh size decreases, the number of elements increases and the von mises stress value changes. At an initial mesh size of 28.5 mm, a von mises stress of 0.043276 MPa was obtained; this value then increased significantly at mesh sizes of 26 mm and 23.5 mm, indicating that the simulation results are still influenced by the mesh size. Furthermore, at a mesh size of 21 mm, the stress changes began to show a stable trend with an error difference of 5.65%. When the mesh size was reduced to 19 mm, the error difference decreased to 1.17%, which is below the general tolerance limit of 5%. This indicates that the simulation results have reached a convergent state, which is also evident in the grid independence test graph that begins to flatten in Figure 8. Therefore, the 19 mm mesh size was selected as the optimal mesh because it provides stable results with a good level of accuracy while still considering computational efficiency.

P-ISSN: 1411-3414
E-ISSN: 2549-9815

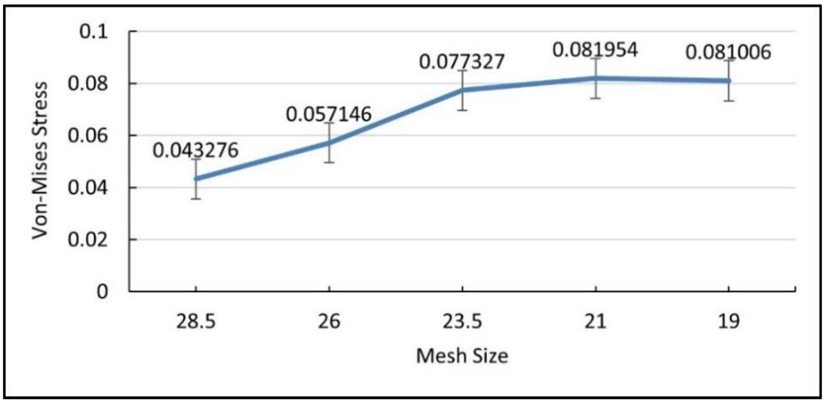

Figure 8. Graph of Grid Independence Test (Convergence)

2.7 Validation of Simulation Results

The results were validated by comparing the von mises stress values obtained from two finite element analysis software packages, namely ANSYS mechanical and solidworks simulation (Figure 9). The purpose of this process was to ensure the consistency and reliability of the numerical simulation results. The tests were performed on the same model with three aspect ratio variations, namely B.1 (AR = 0.8), B.2 (AR = 1), and B.3 (AR = 1.3), with identical loading conditions and material properties in both software programs. To ensure a consistent basis for comparison, the numerical data were extracted from the same location or critical point on the model in both software environments. This approach minimizes discrepancies caused by differences in result interpretation and ensures that the comparison reflects the same stress concentration region. The results of the comparison are presented in Table 9.

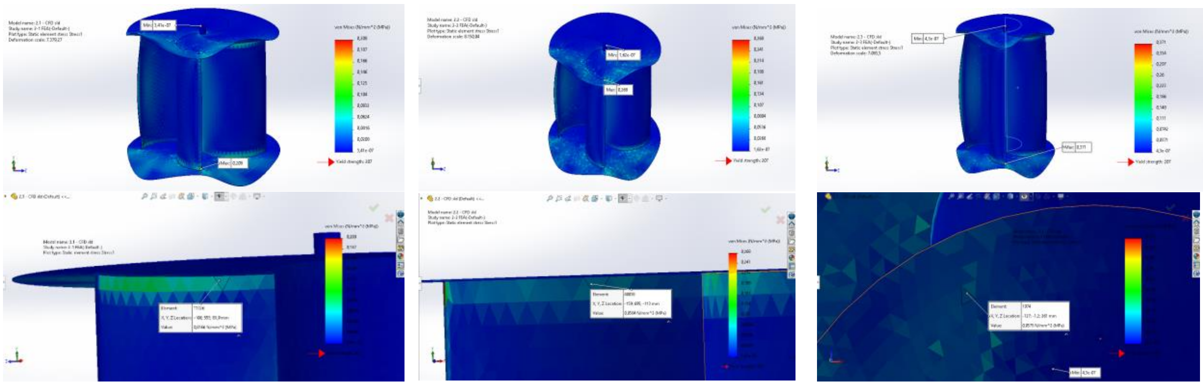

(a) (b) (c)

Figure 9. Von Mises Stress in Turbine Design Using SolidWorks Software; (a) B.1 (AR = 0,8), (b) B.2 (AR = 1), (c) B.3 (AR = 1,3)

The comparison of von mises stress values between ANSYS and SolidWorks for each aspect ratio variation shows relatively small differences. For variation B.1 (AR = 0.8), the error difference was 3.69%; for B.2 (AR = 1), it was 3.56%; and for B.3 (AR = 1.3), it was 1.72%. All of these error values are below the general tolerance limit of 5%, indicating that the simulation results exhibit a good level of agreement. The minor differences observed are likely due to variations in numerical methods, solver algorithms, and mesh discretization approaches used by each software. These results indicate that the ANSYS simulation is consistent with SolidWorks, so the von mises stress analysis results can be considered valid and used for further analysis. The comparison results are presented in Table 9 and visualized in Figure 10.

Table 9. Comparison of Von Mises Stress Validation Results Using Ansys and Solidworks

Variable	Variation	Von Mises Stress (MPa)		Percentage Error (%)
		Ansys	Solidworks	

P-ISSN: 1411-3414
E-ISSN: 2549-9815

	B.1	0.8	0.054	0.056	3.69
Aspect Ratio	B.2	1.0	0.056	0.0580	3.56
	B.3	1.3	0.057	0.0575	1.72

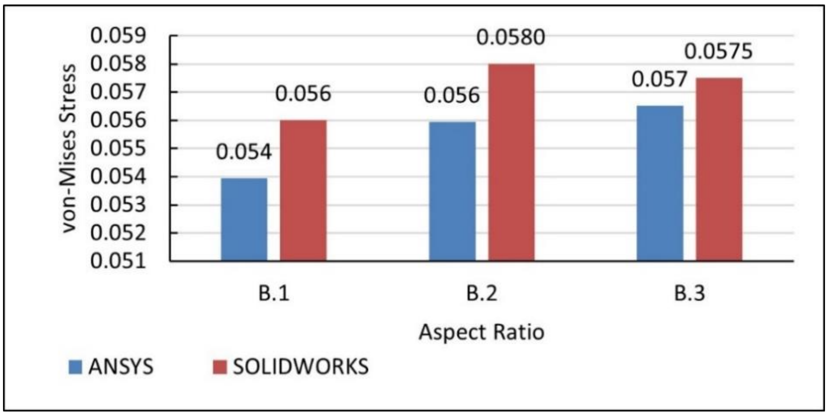

Figure 10. Diagram of Von Mises Stress Validation Analysis Using Ansys and Solidworks

3. Result and Discussion

The structural analysis in this study employs a static structural analysis approach, in which the aerodynamic pressure distribution obtained from CFD simulations is applied as an equivalent static load to the blade structural model. This approach is commonly used in the early stages of design evaluation to determine the distribution of stresses, deformations, and the structural safety factor under maximum loading. Although the aerodynamic forces on turbine blades are inherently dynamic during rotation, the equivalent static load approach can provide a conservative estimate of the maximum structural response that may occur.

To comprehensively analyze the structural response of savonius turbine blades, the results of the finite element analysis (FEA) simulations are visualized in the form of contours of Equivalent von mises Stress, Total Deformation, and Safety Factor for each geometric variation. This visualization covers the blade thickness, aspect ratio, and arc angle parameters, as shown in Figure 11–19. The presentation of these contours aims not only to display the simulation results but also to identify load distributions, stress concentration locations, and deformation patterns resulting from geometric changes. Thus, the analysis is not merely descriptive but also provides a mechanical interpretation of the influence of each geometric parameter on the structural response of the blade.

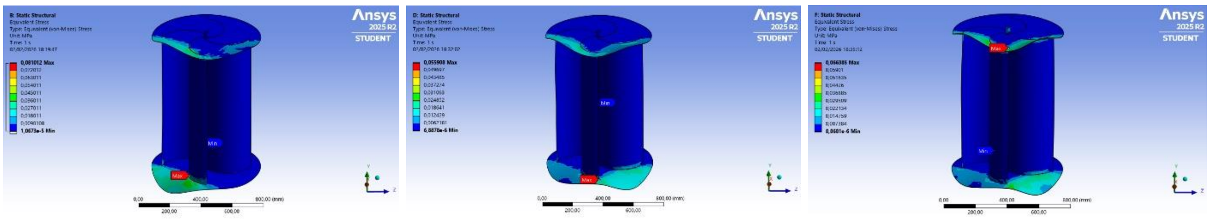

(a) (b) (c)

Figure 11. Equivalent Von Mises Stress in the Geometric Design of the Turbine Blade Thickness. a) 1.2 mm, b) 1.5 mm, c) 2 mm

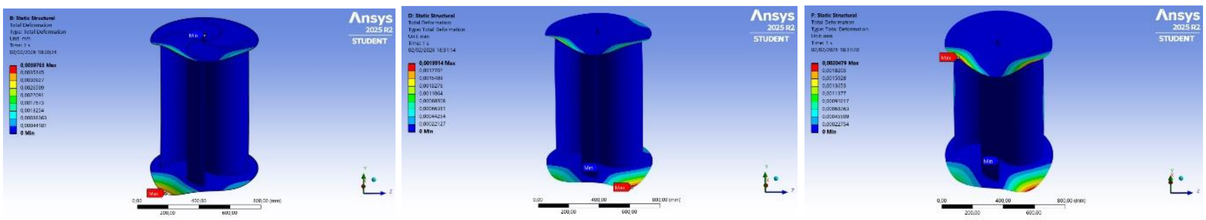

(a) (b) (c)

Figure 12. Total Deformation in the Geometric Design of the Turbine Blade Thickness; a) 1.2 mm, b) 1.5 mm,

c) 2 mm

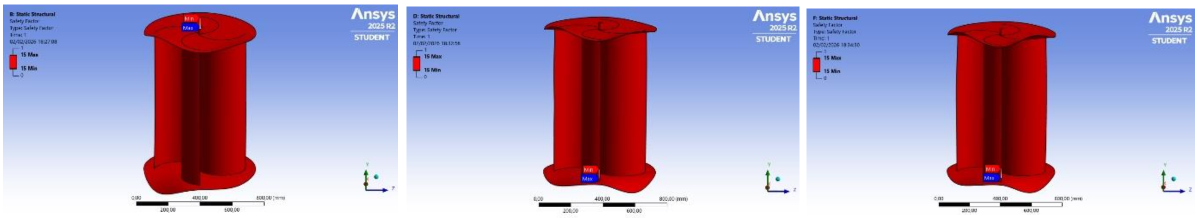

(a) (b) (c)

Figure 13. Safety Factor in Turbine Blade Thickness Geometry Design; a) 1.2 mm, b) 1.5 mm, c) 2 mm

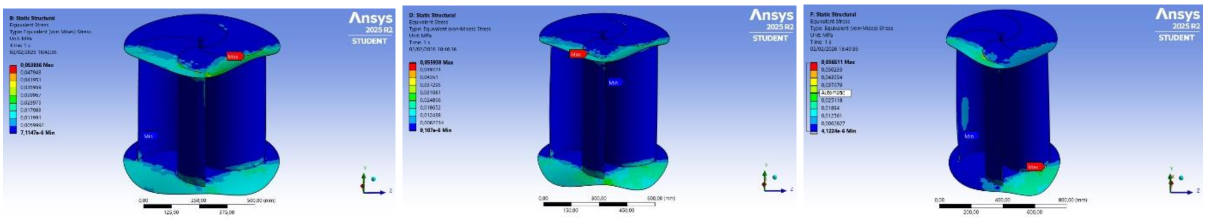

(a) (b) (c)

Figure 14. Equivalent Von Mises Stress in Turbine Aspect Ratio Geometric Design; a) 0.8, b) 1, c) 1.3

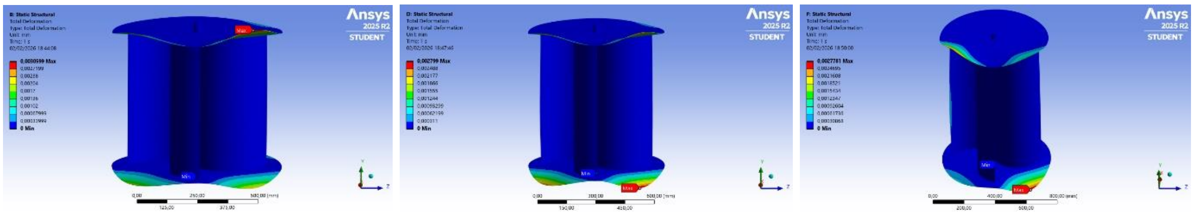

(a) (b) (c)

Figure 15. Total Deformation in Turbine Aspect Ratio Geometry Design; a) 0.8, b) 1, c) 1.3

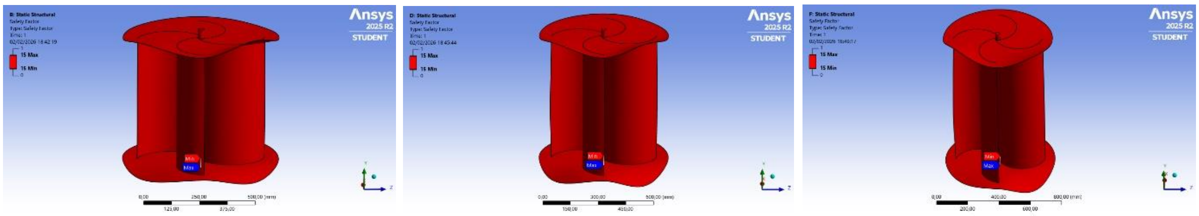

(a) (b) (c)

Figure 16. Safety Factor in Turbine Aspect Ratio Geometric Design; a) 0.8, b) 1, c) 1.3

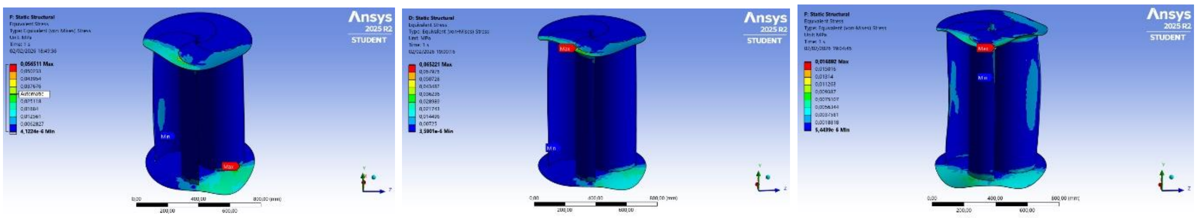

(a) (b) (c)

Figure 17. Equivalent Von Mises Stress in Arc Angle Turbine Geometry Design; a) 120°, b) 150°, c) 180°

P-ISSN: 1411-3414
E-ISSN: 2549-9815

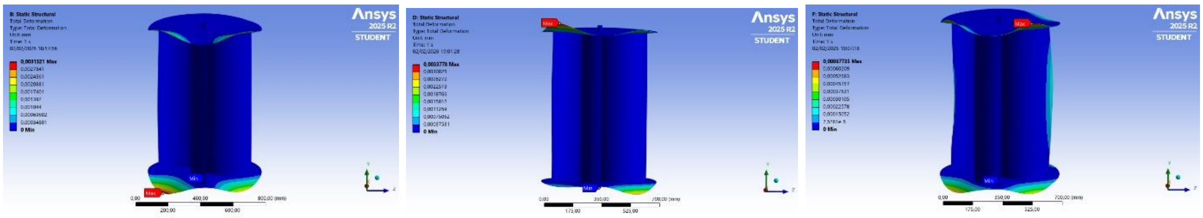

(a) (b) (c)

Figure 18. Total Deformation in the Arc Angle Turbine Geometry Design; a) 120°, b) 150°, c) 180°

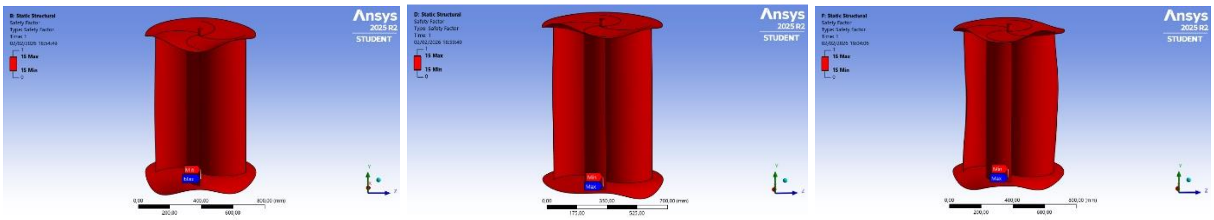

(a) (b) (c)

Figure 19. Safety Factor in Arc Angle Turbine Geometry Design; a) 120°, b) 150°, c) 180°

The results in Table 10 and Figure 20–21 show that the structural response of the blade is influenced not only by the magnitude of the geometric parameters but also by how those geometries govern the load distribution and stress paths within the structure. For variations in thickness, an increase from 1.2 mm to 1.5 mm was found to reduce the maximum stress from 0.081 MPa to 0.056 MPa and decrease the maximum deformation from 3.98×10^{-3} mm to 1.99×10^{-3} mm. However, when the thickness was increased to 2 mm, the maximum stress actually rose again to 0.066 MPa, even though the deformation remained relatively low. This phenomenon indicates that an increase in thickness does not always correlate directly with a decrease in stress, as changes in stiffness also affect the redistribution of loads and internal moments. Consequently, local stress concentrations may occur in certain areas, causing the maximum stress value to increase even though the structure becomes stiffer overall.

Table 10. Finite Element Analysis (FEA) simulation data

Variable	Variation		Von Mises Stress (MPa)			Total Deformation (mm)			FoS
			Min.	Max.	Avg.	Min.	Max.	Avg.	
Blade Thickness	A.1	1.2 mm	1.07E-05	0.081	2.52E-03	0	3.98E-03	8.21E-05	15
	A.2	1.5 mm	6.89E-06	0.056	1.82E-03	0	1.99E-03	5.40E-05	15
	A.3	2.0 mm	8.87E-06	0.066	2.55E-03	0	2.05E-03	8.70E-05	15
Aspect Ratio	B.1	0.8	7.1147E-06	0.054	2.93E-03	0	3.06E-03	9.62E-05	15
	B.2	1.0	9.11E-06	0.056	2.81E-03	0	2.80E-03	8.95E-05	15
	B.3	1.3	4.1224E-06	0.057	2.13E-03	0	2.78E-03	6.89E-05	15
Arc Angle	C.1	120°	1.31E-05	0.055	2.50E-03	0	3.13E-03	1.00E-04	15
	C.2	150°	3.59E-06	0.065	2.29E-03	0	3.38E-03	7.01E-05	15
	C.3	180°	5.44E-06	0.017	8.70E-04	0	6.77E-04	2.75E-05	15

In the aspect ratio variation, an increase in the value from 0.8 to 1.3 resulted in a rise in maximum stress from 0.054 MPa to 0.057 MPa, while maximum strain actually decreased from 3.06×10^{-3}mm to 2.78×10^{-3}mm. This indicates that changes in the blade's geometric proportions increase the moment arm relative to the aerodynamic load, resulting in a larger bending moment and consequently higher stress. On the other hand, a more elongated geometric configuration also increases structural stiffness in certain directions, thereby better resisting global deformation. Thus, there is a trade-off between increased local stress and reduced deformation, which must be considered in the design optimization process.

The most significant effect was observed in the variations in arc angle, where the 180° angle produced the lowest maximum stress of 0.017 MPa and the smallest maximum deformation of 6.77×10^{-4}mm compared to the other variations. Mechanically, increasing the arc angle expands the area capturing

P-ISSN: 1411-3414
E-ISSN: 2549-9815

aerodynamic loads, resulting in a more even pressure distribution along the blade surface. This condition reduces stress concentration caused by sharp pressure gradients, thereby significantly suppressing peak stress. Conversely, at smaller angles such as 120° and 150°, the load distribution tends to be more concentrated in specific areas, increasing the likelihood of higher local stresses. Therefore, it can be concluded that the arc angle parameter plays a dominant role in controlling load distribution and determining the overall structural response of the blade, compared to other geometric parameters.

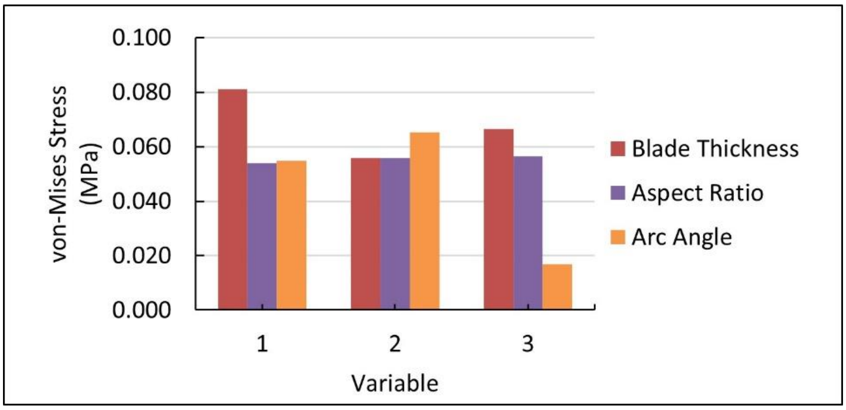

Figure 20. Graph of Analysis Results of Maximum Equivalent Von Mises Stress from FEA Simulation

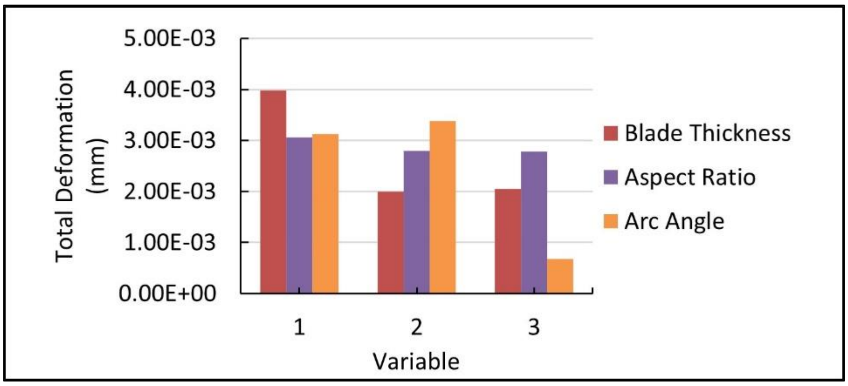

Figure 21. Graph Analysis of the Maximum Total Deformation Results of the FEA Simulation

The simulation results show that all blade geometry variations analyzed yield relatively low stress and strain values with a high safety factor. This indicates that the proposed blade configuration remains within safe limits when subjected to aerodynamic loads under the analyzed operating conditions. High safety factor values do not necessarily indicate that the applied loads are too light; rather, they indicate that the selected combination of blade geometry and material possesses sufficient structural strength for the targeted operating conditions. Thus, the results of this study can provide a basis for safe design and serve as an initial reference for the fabrication process of small-scale savonius turbines as well as for further research and development.

Regarding the possibility of testing under stronger wind conditions, it should be noted that the scope of this study is limited to the structural analysis of turbine blades under low wind speed conditions that are most representative of the operating environment under investigation. This study is a numerical simulation aimed at supporting the development of realistic blade designs that can be fabricated at the laboratory prototype scale. Therefore, the loading conditions are focused on the wind speed range most relevant to the design objectives of savonius turbines for small-scale applications. Testing under higher wind speeds or extreme conditions could be a direction for further research to evaluate structural durability under more severe operating conditions. Additionally, analyses considering transient or cyclic loading, such as material fatigue analysis, have the potential to provide a deeper understanding of long-term structural behavior; however, such analyses are beyond the scope of this study.

P-ISSN: 1411-3414
E-ISSN: 2549-9815

4. Conclusion

This study confirms that the Finite Element Analysis (FEA) approach is an effective and reliable method for evaluating the structural response of savonius turbine blades under aerodynamic loads. The simulation results show that geometric parameters have a dominant influence on stress distribution, deformation, and overall structural performance. Quantitatively, increasing the blade thickness from 1.2 mm to 1.5 mm reduces the maximum stress from 0.081 MPa to 0.056 MPa and the deformation from 3.98×10^{-3} mm to 1.99×10^{-3} mm. However, further increasing the thickness to 2 mm leads to a rise in stress to 0.066 MPa, indicating a non-linear response. Increasing the aspect ratio (0.8 to 1.3) increases stress due to higher bending moments, but reduces deformation, reflecting an increase in global structural stiffness. The arc angle variation is the most significant, where the 180° configuration produces the lowest stress (0.017 MPa) and deformation (6.77×10^{-4} mm) through a more uniform load distribution. Although all configurations show a factor of safety (FoS) of 15, the design evaluation is determined by the stress and deformation response. These findings confirm that optimizing the arc angle is a key strategy for improving blade structural performance. The limitation of this study lies in the use of static assumptions, therefore future research needs to integrate dynamic analysis, experimental validation, and fluid–structure interaction to improve accuracy under real operating conditions.

References

[1] P. W. Andianti and Yushardi, "Potensi Pembangkit Listrik Tenaga Angin Sebagai Alternatif Penerangan Jalan Di Pantai Bambang Kabupaten Lumajang," *Pariwisata Budaya: Jurnal Ilmiah Agama Dan Budaya*, vol. 7, no. 2, pp. 123–130, 2022.

[2] R. P. Simamora, Handarto, and M. Saukat, "Analysis Of Wind Energy Potentials And Technical Analysis Of Wind Turbine To Generate Electricity (A Case Study At Gunung Kincir, Desa Ciheras Kecamatan Cipatujah Kabupaten Tasikmalaya)," in *In Prosiding-Seminar Nasional Teknik Elektro UIN Sunan Gunung Djati Bandung*, Sumedang: SENTER 2019: Seminar Nasional Teknik Elektro, 2019, pp. 91–100. Accessed: Jan. 28, 2026. [Online]. Available: https://senter.ee.uinsgd.ac.id/repositori/index.php/prosiding/article/view/senter2019p12/114

[3] International Renewable Energy Agency (IRENA), "Indonesia Energy Transition Outlook," Masdar, 2022.

[4] M. Usman, K. Kadaryono, M. Dwi Hariska, and M. Ali, "Perencanaan Lampu Penerangan Jalan Menggunakan Turbin Angin Sumbu Vertikal Savonius," *Jurnal FORTECH*, vol. 4, no. 2, pp. 18–25, Dec. 2023, doi: 10.56795/fortech.v4i2.4204.

[5] A. Fadllullah, S. Riyanto, J. Amal Lama No, and K. Tarakan, "POWER DENSITY (STUDI KASUS: KOTA TARAKAN)," *JURNAL INOVTEK POLBENG*, vol. 09, no. 01, pp. 129–137, 2019, Accessed: Jan. 28, 2026. [Online]. Available: https://www.neliti.com/publications/466994/pengembangan-aplikasi-analisis-potensi-angin-sebagai-sumber-energi-terbarukan-me.

[6] J. Victor Tuapetel, I. Arif Triprayoga, and P. M. Santika, "ANALISIS DAN PENGUJIAN Victor KINERJA TURBIN ANGIN SAVONIUS 4 SUDU," *JURNAL TEKNIK MESIN*, vol. 3, no. 2, pp. 46–52, 2019.

[7] N. Ismail and S. Chorul, "RANCANG BANGUN KINCIR ANGIN PEMBANGKIT TENAGA LISTRIK SUMBU VERTIKAL SAVONIUS PORTABEL MENGGUNAKAN GENERATOR MAGNET PERMANEN," *INDUSTRI INOVATIF*, pp. 19–24, 2015 [In Bahasa].

[8] A. Shuhufam and T. Y. Yuwono, "Studi Eksperimen Peningkatan Kinerja Turbin Angin Savonius Dengan Penempatan Silinder Sirkular Didepan Returning Blade Turbin Turbin pada Jarak S/D = 2,6," *JURNAL TEKNIK ITS*, vol. 9, no. 2, 2020 [In Bahasa].

[9] R. S. Afiatullah and P. Elmiawan, "ANALISIS TEGANGAN STATIC PADA PERANCANGAN MESIN REWINDING LINER MENGGUNAKAN METODE FINITE ELEMENT ANALYSIS," vol. 3, no. 1, Mar. 2023.

[10] H. Permana, W. Dwi Prasetyo, D. Hermawan, and T. Farudin, "KEKUATAN SUDU TURBIN

P-ISSN: 1411-3414
E-ISSN: 2549-9815

ANGIN SAVONIUS DENGAN ANALISA ELEMEN HINGGA SAVONIUS WIND TURBINE BLADE POWER WITH FINITE ELEMENT ANALYSIS," *Jurnal Baut dan Manufaktur*, vol. 5, no. 2, pp. 46–56, 2023.

[11] S. Putraji, A. P. Tetuko, and Djuhana, "Simulasi Kekuatan Mekanik Sudu Turbin Angin Sumbu Horizontal Menggunakan Bahan Steel," *Journal of Technical Engineering: Piston*, vol. 4, no. 2, pp. 71–76, 2021.

[12] F. Sutanto, A. Wicaksana, D. Anggito, and P. Tetuko, "Analisa Distribusi Stress dan Displacement pada Sudu Turbin Angin Savonius dengan Material Baja Menggunakan Simscale," *Journal of Technical Engineering: Journal of Technical Engineering: Piston*, vol. 4, no. 2, pp. 56–63, 2021.

[13] Z. B. Caniago, "Kecepatan Korosi Oleh 3 Bahan Oksidan Pada Plat Besi," *GRADIEN: Jurnal Ilmiah MIPA*, vol. 2, no. 2, pp. 161–166, 2006.

[14] Martinus, M. D. Susila, and M. Budiyono, "Analisis Fenomena Penampang Alir Vertical Axis Wind Turbine (VAWT) Tipe Heliks Terhadap Kecepatan Angin Sebagai Pembangkit Listrik Alternatif Berskala Rumah Tangga," *Jurnal Mechanical*, vol. 2, no. 2, pp. 1–10, Sep. 2011.

[15] Sutarno, *Sumber Daya Energi*. Yogyakarta: Graha Ilmu, 2013.

[16] J. Sargolzaei, "Prediction of the power ratio in wind turbine Savonius rotors using artificial neural networks," *INTERNATIONAL JOURNAL OF ENERGY AND ENVIRONMENT*, vol. 1, no. 2, pp. 51–56, 2007.

[17] U. S. Dharma and M. Masherni, "Pengaruh Desain Sudu Terhadap Unjuk Kerja Prototype Turbin Angin Vertical Axis Savonius," *Turbo : Jurnal Program Studi Teknik Mesin*, vol. 5, no. 2, pp. 138–148, Sep. 2017, doi: 10.24127/trb.v5i2.246.

[18] U. Mulyo Sugeng and V. Hadi, "Analisis Perbandingan 2 Dan 3 Blade Turbin Angin Kecil Sumbu Vertikal Tipe Savonius," *Sainstech*, vol. 32, no. 4, pp. 1–11, Dec. 2023, Accessed: Jan. 28, 2026. [Online]. Available: https://journal.istn.ac.id/index.php/sainstech/article/view/1749/1150 .

[19] Vinit. V Bidi, Devendrappa M. K., Chandan S. P, Arun J. P., and Maruthi G.V., "Highway Power Generation using Low Cost Vertical Axis Wind Turbine [VAWT]," *International Journal of Engineering Science and Computing*, vol. 7, no. 5, pp. 12008–12012, Apr. 2017, [Online]. Available: https://api.semanticscholar.org/CorpusID:212608515

[20] S. Novita, E. Ginting, and W. Astuti, "Analisis Laju Korosi dan Kekerasan pada Stainless Steel 304 dan Baja Nikel Laterit dengan Variasi Kadar Ni (0, 3, dan 10%) dalam Medium Korosif," *JURNAL Teori dan Aplikasi Fisika*, vol. 06, no. 01, pp. 21–31, Jan. 2018.

[21] Sumarji, "STUDI PERBANDINGAN KETAHANAN KOROSI STAINLESS STEEL TIPE SS 304 DAN SS 201 MENGGUNAKAN METODE U-BEND TEST SECARA SIKLIK DENGAN VARIASI SUHU DAN PH," *ROTOR*, vol. 4, no. 1, pp. 1–8, Jan. 2011.

[22] I. Nurcholis, W. D. Pratiwi, M. K. Al Amin, D. Anggara, and E. Wahyu R. W., "Analisis komparasi kekerasan dan struktur mikro lasan dissimilar material pada berbagai posisi pengelasan di industri fabrikasi," *Journal of Welding Technology*, vol. 4, no. 1, pp. 1–8, Jun. 2022, doi: http://dx.doi.org/10.30811/jowt.v4i1.2967.

[23] A. Rimmon, D. Leni, I. Alghani, Y. Vadila, and R. Stevano, "ANALYSIS OF SAVONIUS TURBINE BLADES WITH ANGLE VARIATIONS USING FEA SIMULATION IN SOLIDWORKS," in *The 5th International Conference on Innovations in Social Sciences Education and Engineering (ICoISSEE-5)*, Bandung: The Fifth International Conference on Innovations Social Sciences Education and Engineering, Jul. 2025, pp. 1–11. Accessed: Jan. 29, 2026. [Online]. Available: https://conference.loupiasconference.org/index.php/ICoISSEE-5/article/view/691

[24] G. R. Liu and S. S. Quek, *The finite element method: A practical course, Second Edition*, Second Edition. Oxford: Butterworth-Heinemann (an imprint of Elsevier Science Ltd), 2013.

P-ISSN: 1411-3414
E-ISSN: 2549-9815

[25] R. C. Hibbeler, *Mechanics of Materials 9th Edition*, 9th Edition. New Jersey: Pearson Prentice Hall, 2014.

[26] I. N. Agus Adi, K. R. Dantes, and I. N. P. Nugraha, "ANALISIS TEGANGAN STATIK PADA RANCANGAN FRAME MOBIL LISTRIK GANESHA SAKTI (GASKI) MENGGUNAKAN SOFTWARE SOLIDWORKS 2014," *Jurnal Pendidikan Teknik Mesin Undiksha*, vol. 6, no. 2, p. 113, Aug. 2018, doi: 10.23887/jjtm.v6i2.13046.

[27] L. A. N. Wibawa, "Simulasi umur fatik rangka main landing gear menggunakan metode elemen hingga," *Ansys Dinamika Teknik Mesin*, vol. 10, no. 2, pp. 120–126, 2020, doi: 10.29303/dtm.v10i2.337.

[28] R. C. Hibbeler, *Mechanics of Materials Vol.8*, vol. 8. Pearson Prentice Hall, 2011.

[29] T. Mulyanto and A. D. Sapto, "ANALISIS TEGANGAN VON MISES POROS MESIN PEMOTONG UMBI-UMBIAN DENGAN SOFTWARE SOLIDWORKS," *PRESISI*, vol. 18, no. 2, pp. 24–29, Jul. 2017.

[30] H. Habibie, R. Lapisa, I. Irzal, and Z. Abadi, "Rancang Bangun dan Analisis Kinerja Turbin Angin Sumbu Vertikal Modifikasi Menggunakan Empat Buah Blade," *MASALIQ*, vol. 4, no. 1, pp. 445–455, Jan. 2024, doi: 10.58578/masaliq.v4i1.2668.

[31] P. Chairany and Sugiyanto, "RANCANG BANGUN TURBIN ANGIN SUMBU VERTIKAL TIPE SAVONIUS UNTUK SISTEM PENERANGAN PERAHU NELAYAN," *Jurnal Rekayasa Mesin*, pp. 59–64, 2016, doi: https://doi.org/10.32497/rm.v11i2.531.

[32] H. Rohman, "Rancang Bangun Pembangkit Listrik Tenaga Angin Menggunakan Turbin Angin Savonius," Jember, 2019.

[33] P. Parta, R. Rofiroh, and A. G. Fatria, "RANCANG BANGUN TURBIN ANGIN SAVONIUS POROS VERTIKAL DENGAN KINCIR 4 SUDU SEBAGAI PEMBANGKIT LISTRIK PADA PENERANGAN JALAN RAYA," *Motor Bakar : Jurnal Teknik Mesin*, vol. 4, no. 2, pp. 1–5, Aug. 2020, doi: 10.31000/mbjtm.v4i2.5750.

[34] M. F. Haq and Mar'ana, *RANCANG BANGUN TURBIN SAVONIUS PENGGERAK POMPA SUBMERSIBLE SEBAGAI ALAT PENYIRAM TANAMAN BERBASIS ARDUINO*. Makassar: Politeknik Negeri Ujung Pandang, 2023.

[35] A. Laka, D. N. Ully, P. Ginting, Nasaruddin, D. M. Para, and B. S. Wuwur, "Rancang Bangun Turbin Angin Savonius Tiga Sudu untuk Dimanfaatkan sebagai Penerangan bagi Masyarakat di Daerah Terpencil," *JURNAL FLYWHEEL*, vol. 15, no. 1, pp. 35–43, Feb. 2024, doi: 10.36040/flywheel.v15i1.8749.

[36] M. I. Nadhief, S. Hadi, and D. D. Prija Tjahjana, "STUDI EKSPERIMENTAL PENGARUH VARIASI SUDUT BLADE ARC TERHADAP PERFORMA SAVONIUS HORIZONTAL AXIS WATER TURBINE TIPE L PADA ALIRAN DALAM PIPA," *Mekanika: Majalah Ilmiah Mekanika*, vol. 18, no. 2, pp. 35–38, Nov. 2019, doi: 10.20961/mekanika.v18i2.35402.

[37] A. Alaimo, A. Esposito, A. Milazzo, C. Orlando, and F. Trentacosti, "Slotted Blades Savonius Wind Turbine Analysis by CFD," *Energies (Basel).*, vol. 6, no. 12, pp. 6335–6351, Dec. 2013, doi: 10.3390/en6126335.